Impact of ^{99m}Tc-GSA SPECT Image-Guided Inverse Planning on Dose–Function Histogram Parameters for Stereotactic Body Radiation Therapy Planning for Patients With Hepatocellular Carcinoma: A Dosimetric Comparison Study

Ryo Toya[1] 🔘, Tetsuo Saito[1], Yudai Kai[2], Shinya Shiraishi[3], Tomohiko Matsuyama[1], Takahiro Watakabe[1], Fumi Sakamoto[3], Noriko Tsuda[3], Yoshinobu Shimohigashi[2], Yasuyuki Yamashita[3], and Natsuo Oya[1]

Abstract

Purpose: To evaluate the impact of ^{99m}Tc-labeled diethylene triamine pentaacetate-galactosyl human serum albumin (^{99m}Tc-GSA) single-photon emission computed tomography (SPECT) image-guided inverse planning on the dose–function histogram (DFH) parameters for stereotactic body radiation therapy planning in patients with hepatocellular carcinoma (HCC).

Methods: Eleven patients were enrolled in this study. The functional liver structure (FLS) was derived from SPECT thresholds of 60% to 80% of the maximum pixel value. Two treatment plans optimized without FLS (plan C) and with FLS (plan F) were designed for 50 Gy to the planning target volume (PTV). The DFH parameters were calculated as follows: $Fx =$ (sum of the counts within the liver volume receiving a dose $>x$ Gy/sum of the counts within the whole liver volume) $\times$ 100. Other parameters for the PTV included D_{95}, mean dose, conformity index (CI), and homogeneity index (HI).

Results: Compared with plan C, plan F significantly reduced DFH parameters of F_5 to F_{40} ($P < .05$). There were no significant differences in the parameters of the PTV of D_{95}, mean dose, CI, and HI and organs at risks (stomach, duodenum, spinal cord, and kidneys) between plans C and F.

Conclusion: DFH analyses revealed that ^{99m}Tc-GSA SPECT image-guided inverse planning provided dosimetric benefits related to sparing of liver function and may reduce hepatic toxicities.

Introduction

Stereotactic body radiation therapy (SBRT) for hepatocellular carcinoma (HCC) has been widely performed as an alternative to standard treatments, such as surgical resection and radio-frequency ablation (RFA).[1] The SBRT delivers a highly conformal potent dose of radiation to the tumor in some fractions while minimizing radiation damage to organs at risk (OARs). It provides excellent local control for HCC with a reported control rate of 80% to 90%.[2-4] However, radiation-induced liver injury (RILI), which occurs in 10% to 20% of patients with

[1] Department of Radiation Oncology, Kumamoto University Hospital, Kumamoto, Japan
[2] Department of Radiological Technology, Kumamoto University Hospital, Kumamoto, Japan
[3] Department of Diagnostic Radiology, Kumamoto University Hospital, Kumamoto, Japan

Corresponding Author:
Ryo Toya, Department of Radiation Oncology, Kumamoto University Hospital, 1-1-1 Honjo, Chuo-ku, Kumamoto 860-8556, Japan.
Email: ryo108@kumamoto-u.ac.jp

HCC undergoing SBRT, remains a problematic adverse effect because of preexisting liver dysfunctions occurring secondary to comorbid conditions, such as hepatitis B and C infection and cirrhosis.[3,4] Because the HCC response to radiation therapy (RT) exhibits a dose–response relationship,[5] a sophisticated RT technique is required to deliver a sufficient RT dose to control the HCC while preventing RILI. Intensity-modulated radiotherapy (IMRT) based on inverse planning using a dose–volume histogram (DVH) is becoming more widely applied for the treatment of HCC.[6] Some planning studies have suggested that the use of IMRT yielded dosimetric benefits for the target volume coverage and sparing of the liver superior to those of 3-dimensional conformal RT.[6] However, because DVH is estimated on the basis of computed tomography (CT) images, which provide only morphological information, inhomogeneity of liver function is not considered in planning.[7]

A radiopharmaceutical tracer, ^{99m}Tc-labeled diethylene triamine pentaacetate-galactosyl human serum albumin (^{99m}Tc-GSA), that binds specifically to the hepatic asialoglycoprotein receptor is used to assess hepatic function.[8] Single-photon emission computed tomography (SPECT) using ^{99m}Tc-GSA provides 3-dimensional information about regional liver function, and its findings suggest that regional function of patients with liver tumors is inhomogeneous because of previous treatments, such as RFA and transarterial chemoembolization (TACE).[7] A recent study revealed that a dose–function histogram (DFH) using ^{99m}Tc-GSA SPECT provides dosimetric information of the liver function of patients with HCC who underwent SBRT.[7] Introduction of functional information of ^{99m}Tc-GSA SPECT for use in inverse planning for IMRT might be a reasonable approach to spare liver function. We evaluated the impact of ^{99m}Tc-GSA SPECT image-guided inverse planning on the DFH parameters of SBRT planning in patients with HCC.

Materials and Methods

Patients

This retrospective planning study is the secondary analysis of our previous study[7] and is based on prospectively acquired imaging data in a part of another prospective study of SBRT for HCC. This study received institutional review board approval (No. 1395), and written informed consent for the future use of images in this study was obtained from all patients. Between August 2013 and February 2017, 12 consecutive patients with HCC received SBRT in our institution. Of these 12 patients, 11 were included in this study; 1 patient was excluded because he received SBRT for the recurrent lesion on the surface of the liver after surgery. The patient and tumor characteristics are summarized in Table 1. Eight patients (73%) had undergone previous treatment for lesions other than SBRT-treated lesions in the liver or remnant liver; RFA in 5, percutaneous ethanol injection therapy in 1, and TACE in 6, respectively. No patient received SBRT before treatment. All

Table 1. Patient and Tumor Characteristics.

| Characteristics	n
Age (years)	Median: 69 (range: 58-76)
Sex	
Male	9
Female	2
Hepatitis virus infection	
HBV	3
HCV	4
None	4
Child-Pugh class	
A	7
B	4
T stage (UICC 7th)	
T1	10
T2	1
Previous treatment for other lesions	
Yes	8
No	3
Tumor location	
S1	3
S4	3
S5	2
S8	3
GTV (cm3)	Median: 9.3 (range: 2.3–21.1)
PTV (cm3)	Median: 42.9 (range: 22.4–81.3)

Abbreviations: GTV, gross tumor volume; HBV, hepatitis B virus; HCV, hepatitis C virus; PTV, planning target volume; UICC, Union for International Cancer Control.

patients underwent ^{99m}Tc-GSA SPECT/CT imaging within 1 month before SBRT planning.

Fusion of the SPECT/CT and Planning Simulation CT Images

The details of generating fused SPECT/CT images and planning simulation CT are described elsewhere.[7,9] We used a SPECT/CT system (Symbia T16; Siemens Healthcare, Erlangen, Germany) for the SPECT/CT imaging. Hepatic SPECT data (60 steps of 15 seconds per step, 360°, 128 × 128 matrix) were obtained over 20 to 35 minutes after the intravenous injection of ^{99m}Tc-GSA (185 MBq). To enable SPECT attenuation correction, noncontrast-enhanced helical CT images (matrix, 512 × 512 pixels; slice thickness, 2 mm; and slice interval, 2 mm) were obtained. After registration between SPECT and CT images, a CT-derived attenuation-coefficient map was created. For SPECT reconstruction, the ordered-subset expectation maximization algorithm (Flash 3D; Siemens Healthcare) was applied.

For the planning simulation CT acquisition, we used a Light-Speed real-time (RT) CT scanner (GE Medical Systems, Waukesha, Wisconsin). Patients lay supine, and abdominal compression was applied. Immediately after a dynamic contrast-enhanced scan, a nonhelical slow-speed scan with a gantry rotation time of 4 seconds, slice thickness of 2.5 mm, and slice interval of 2.5 mm was performed under free breathing.
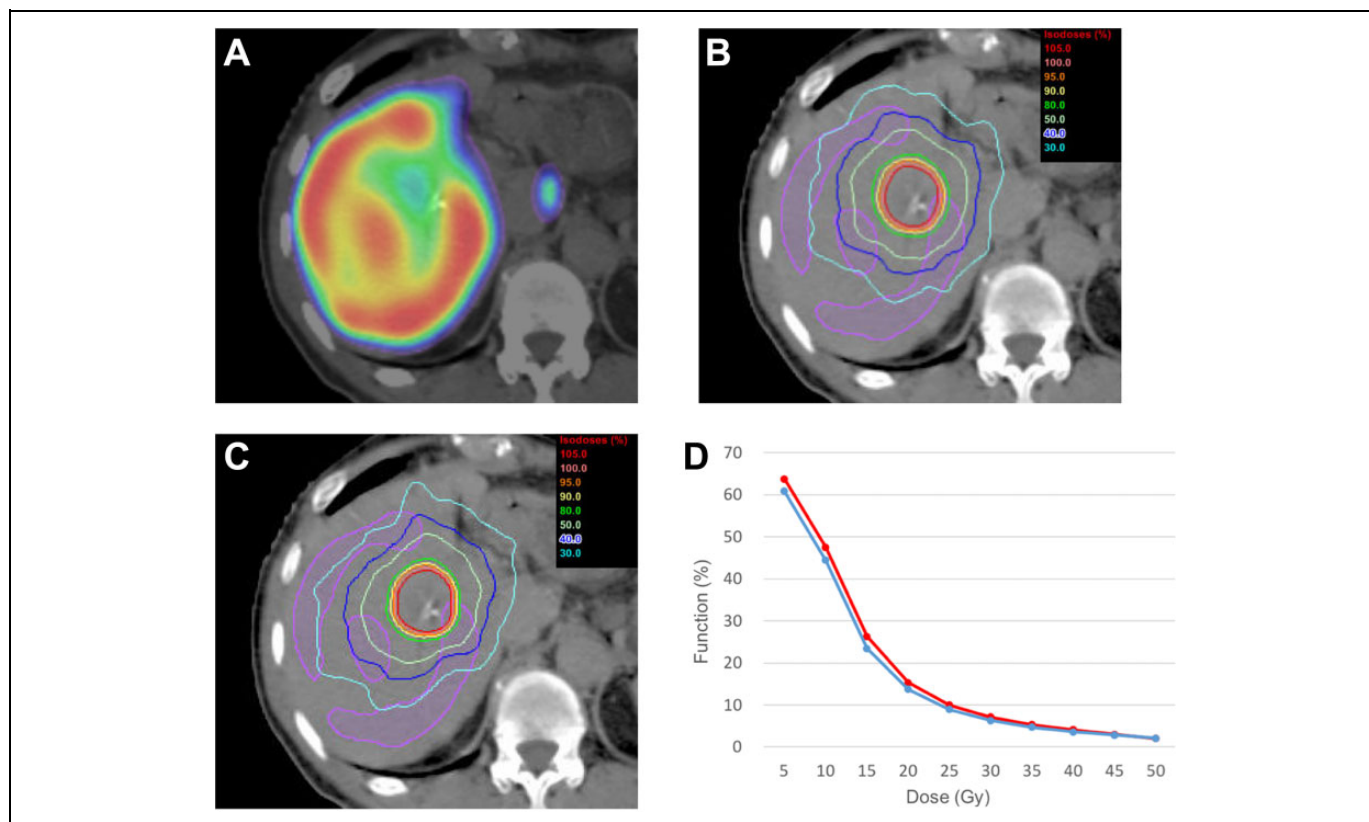
Figure 1. Patient with recurrent hepatocellular carcinoma in segment 5. He received multiple surgical treatments, transarterial chemoembolization, and radiofrequency ablation. A, Fused images from single-photon emission computed tomography (SPECT) and planning computed tomography. The SPECT image shows the inhomogeneity of the liver function. B, Dose distributions of the conventional plan (plan C) optimized without functional liver structure (FLS). C, Dose distributions of the functional image-guided plan (plan F) optimized with FLS. The FLS (purple) was derived from SPECT thresholds equal to 80% of the maximum pixel value. D, The dose–function histogram of plan C (red) and plan F (blue).

Attenuation-corrected SPECT and CT images and planning CT images were transferred to a Velocity AI (version 3.0.2; Varian Medical Systems, Palo Alto, California). After registration between the SPECT and CT images by hardware arrangement, we registered the SPECT/CT images onto the planning CT images: a rigid image registration followed by a nonrigid deformable registration. During this process, each SPECT voxel was mapped to a new position based on the transformations used in the CT–CT registration, resulting in new SPECT/CT fused images that were deformably registered with the planning CT images (planning SPECT/CT images).

Construction of the Functional Liver Structure

The functional liver structure (FLS) as an avoidance structure for optimization in inverse planning was derived from SPECT thresholds of the 60% to 80% of maximum pixel value.[10] The threshold level was preferred to create a gap of the FLS around the target volumes (Figure 1).

Treatment Planning

Planning CT images and the FLS were transferred to the Eclipse RT planning system (version 10.0; Varian Medical

Systems). The structures of the target and OARs were delineated on the basis of the planning CT images.

We defined the gross tumor volume (GTV) as the primary tumor evident on contrast-enhanced CT and/or magnetic resonance (MR) images. The clinical target volume margin of 0 to 5 mm was added to the GTV for subclinical invasion. The planning target volume (PTV) margins of 10 mm for the superior–inferior and 5 mm for the left–right and anterior–posterior directions were added to cover the respiratory motions and setup errors.[9,11] The SBRT plans were designed to use RapidArc with 6 MV photons generated by a linear accelerator (Clinac iX; Varian Medical Systems). The plan was generated by using 2 arcs rotating from 181° to 179° clockwise and from 179° to 181° anticlockwise with the dose rate varied between 0 and 600 MU/min. The total prescribed dose was 50 Gy in 5 fractions. We created 2 RT plans: a plan optimized without FLS (conventional plan: plan C) and a plan optimized with FLS (functional image-guided plan: plan F). The dose constraints for optimization of the target volumes and OARs are shown in Table 2. As there were no established dose constraints for the structures, we simplified and modified the previous planning study based on the FLS defined by MR imaging using gadolinium–ethoxybenzyl–diethylenetriamine pentaacetic acid

Table 2. Dose Constraints for the Conventional and Functional Image-Guided Inverse Plans.

Structure	Conventional Plan (Plan C)			Functional Image-Guided Plan (Plan F)		
	Dose (cGy)	Volume (%)	Priority	Dose (cGy)	Volume (%)	Priority
PTV	6000	1	70	6000	1	70
	4750	95	100	4750	95	100
Liver—GTV	2000	20	100	2000	20	100
Functional liver—GTV	NA			1500	15	100
Spinal cord	2500	0	20	2500	0	20
Stomach	2500	0	20	2500	0	20
Duodenum	2500	0	20	2500	0	20
Right kidney	2500	10	10	2500	10	10
Left kidney	2500	10	10	2500	10	10

Abbreviations: GTV, gross tumor volume; NA, not applicable; PTV, planning target volume.

(Gd-EOB-DTPA).[11] V_x means the percentage of the structure volume receiving $>x$ Gy.

Calculating the Parameters of DFH

Planning CT images, delineated structures, and dose distributions were transferred to Velocity AI. After registration between the planning CT images and planning SPECT/CT images by hardware arrangement, we incorporated delineated structures and dose distributions into the planning SPECT/CT images. Structures of the irradiated volumes of the liver parenchyma were generated at 5 Gy dose increments on the basis of the dose distribution information.

DFH parameters for 5 to 50 Gy were calculated as follows[7]:

$$Fx = \frac{\text{sum of the counts within the liver volume receiving a dose of } >x \text{ Gy}}{\text{sum of the counts within the whole liver volume}} \times 100.$$

Data Analysis

The parameters of the DVH of plans C and F were calculated in terms of dose constraints for optimization. DVH parameters of the V_5 to V_{50} and mean dose for the normal liver (liver $-$ GTV) were also calculated. For the PTV, the absorbed dose received by 95% and 98% of the PTV (D_{95} and D_{98}), mean dose, conformity index (CI), and homogeneity index (HI) were used to evaluate the PTV.[12] The CI was calculated as follows:

$$\text{CI} = \frac{V_{\text{Tref}}}{V_T} \times \frac{V_{\text{Tref}}}{V_{\text{ref}}}$$

where V_{Tref} is the volume of the target covered by the reference isodose (100%, 98%, and 95% of the prescribed dose), V_T is the target volume, and V_{ref} is the volume of the reference isodose.

The HI was calculated as follows:

$$\text{HI} = \frac{D_{2\%} - D_{98\%}}{D_{50\%}}$$

where $D_{x\%}$ was the absorbed dose received by $x\%$ of the PTV. For the evaluation of OARs, the maximum dose, mean dose, and/or V_x were employed. The monitor units (MUs) for the 2 plans were also recorded.

The differences in the parameters between the 2 plans were evaluated by using the paired t test. Differences with P values of $<.05$ were considered to be statistically significant. Statistical calculations were performed by using SPSS software, version 24.0 (IBM, Armonk, New York).

Results

The dosimetric parameters are shown in Table 3. In comparison with plan C, plan F significantly reduced the DFH parameters of F_5 to F_{40}, and plan F did not significantly increase F_{45} and F_{50}. There were no significant differences in the DVH parameters of D_{95}, D_{98}, mean dose, CI_{95}, CI_{98}, CI_{100}, and HI for the PTV between plans C and F. Plan F significantly reduced V_5, V_{10}, V_{15}, V_{20}, V_{25}, V_{30}, V_{40}, and the mean dose of the normal liver, and plan F did not significantly increase V_{35}, V_{45}, and V_{50}. There were no significant differences in the parameters of the OARs of the stomach, duodenum, spinal cord, and kidneys between plans C and F. No patient received ≥ 25 Gy to their kidneys. There was no significant difference in the MUs between plans C and F. Figure 1 shows a representative case with parametric discrepancies between plans C and F because of previous treatment.

Discussion

Previous reports of the dosimetric benefit of the use of SPECT images in inverse planning have been focused on treatment using radiopharmaceutical tracers, such as ^{99m}Tc-labeled macroaggregated albumin[13] and ^{99m}Tc-labeled diethylene triamine pentaacetate,[14] of patients with lung cancer. Our study revealed that ^{99m}Tc-GSA SPECT image-guided inverse planning provided a dosimetric benefit of sparing liver function while maintaining coverage of the PTV in patients with HCC. Furthermore, our treatment technique did not increase the DVH parameters of the OARs. Our treatment technique provides a great value especially in cases where the regional function of patients is inhomogeneous due to the previous treatments.[7]

Previous studies have suggested that hepatobiliary phase images acquired by MR imaging using Gd-EOB-DTPA, which is absorbed by hepatocytes, enables evaluation of the functional

Table 3. Dosimetric Parameters Between Conventional and Functional Image-Guided Plans.

	Plan C	Plan F	P Value
DFH parameter			
Liver			
F5 (%)	65.4 ± 9.8	63.9 ± 9.3	.025
F10 (%)	44.9 ± 8.4	42.8 ± 6.5	.025
F15 (%)	24.6 ± 5.7	23.2 ± 4.6	.017
F20 (%)	14.4 ± 3.6	13.7 ± 3.1	.024
F25 (%)	9.3 ± 2.4	8.8 ± 2.2	.030
F30 (%)	6.6 ± 1.8	6.3 ± 1.7	.024
F35 (%)	5.0 ± 1.4	4.8 ± 1.3	.029
F40 (%)	4.0 ± 1.1	3.8 ± 1.1	.026
F45 (%)	3.2 ± 1.0	3.1 ± 1.0	.058
F50 (%)	2.2 ± 1.0	2.2 ± 0.9	.912
DVH parameter			
PTV			
D95 (Gy)	46.9 ± 0.3	46.8 ± 0.3	.520
D98 (Gy)	45.3 ± 0.7	44.7 ± 0.9	.128
Mean dose (Gy)	52.6 ± 1.8	52.4 ± 1.8	.428
CI95	0.87 ± 0.02	0.88 ± 0.02	.094
CI98	0.80 ± 0.06	0.80 ± 0.06	.964
CI100	0.71 ± 0.18	0.71 ± 0.16	.913
HI	0.23 ± 0.05	0.24 ± 0.06	.374
Liver—GTV			
V5 (%)	65.8 ± 9.3	64.3 ± 9.1	.023
V10 (%)	45.0 ± 7.3	43.0 ± 5.8	.035
V15 (%)	25.1 ± 4.2	23.9 ± 3.7	.020
V20 (%)	14.9 ± 2.5	14.3 ± 2.4	.040
V25 (%)	9.7 ± 1.7	9.3 ± 1.7	.029
V30 (%)	6.9 ± 1.3	6.6 ± 1.4	.045
V35 (%)	5.2 ± 1.1	5.0 ± 1.1	.054
V40 (%)	4.1 ± 0.9	3.9 ± 0.9	.031
V45 (%)	3.1 ± 0.8	3.0 ± 0.8	.059
V50 (%)	2.1 ± 0.9	2.0 ± 0.8	.714
Mean dose (Gy)	11.3 ± 1.5	11.0 ± 1.4	.026
Stomach			
Dmax (Gy)	13.8 ± 5.7	13.7 ± 5.7	.552
Duodenum			
Dmax (Gy)	6.5 ± 8.7	6.7 ± 9.0	.416
Spinal cord			
Dmax (Gy)	10.9 ± 3.6	9.9 ± 4.0	.307
Right kidney			
V25 (%)	0	0	1.000
Left kidney			
V25 (%)	0	0	1.000
Monitor unit	609.0 ± 89.9	619.6 ± 78.6	.148

Abbreviations: CI, conformity index; DFH, dose–function histogram; DVH, dose–volume histogram; GTV, gross tumor volume; HI, homogeneity index; PTV, planning target volume.

liver.[15,16] Tsegmed et al[11] performed a planning study using hepatobiliary phase images and inverse planning technique. They defined the FLS as an area of the liver–spleen with a contrast ratio ≥1.5 and analyzed DVH parameters of the FLS. They found that the inverse planning technique achieved a reduced radiotherapeutic dose to the FLS. However, because the definition of the FLS was based on the threshold segmentation technique, which is similar to that for the FLS in our study, inhomogeneity of the function may exist within the FLS, and some function may exist in some part of the whole liver other than the defined FLS. The advantage of the DFH for evaluation of irradiated liver function is that inhomogeneity of liver function within the whole liver is fully considered in the calculation because the DFH calculation is based on the sum of the counts within the whole liver.[7] Our study based on this precise evaluation method of the DFH analysis also revealed that functional image-guided inverse planning reduced the RT dose to the liver function. In the future, technical development of RT planning systems may yield further dosimetric benefits by inverse planning based on dose constraints for not only DVH but also DFH parameters for SBRT planning in the treatment of HCC.

There were some limitations in our study. First, this was only a planning study based on a relatively small number of patients, and we were unable to comment on the optimal SPECT thresholds for yielding FLS or dose constraints for optimization. Second, the accuracy of the deformable registration between the planning CT and SPECT images was not evaluated. Misregistration between these images may have influenced the results of our study. Further prospective clinical trials based on a large patient population and SPECT/CT planning simulation are required to evaluate the clinical benefits of our techniques.

In conclusion, our DFH analyses revealed that ^{99m}Tc-GSA SPECT image-guided inverse planning provided a dosimetric benefit for sparing liver function and may reduce hepatic toxicities.

Declaration of Conflicting Interests

Funding

ORCID iD

Ryo Toya https://orcid.org/0000-0001-9764-5718

References

1. Klein J, Dawson LA. Hepatocellular carcinoma radiation therapy: review of evidence and future opportunities. *Int J Radiat Oncol Biol Phys*. 2013;87(1):22-32.
2. Seo YS, Kim MS, Yoo SY, et al. Preliminary result of stereotactic body radiotherapy as a local salvage treatment for inoperable hepatocellular carcinoma. *J Surg Oncol*. 2010;102(3):209-214.
3. Andolino DL, Johnson CS, Maluccio M, et al. Stereotactic body radiotherapy for primary hepatocellular carcinoma. *Int J Radiat Oncol Biol Phys*. 2011;81(4):e447-e453.
4. Sanuki N, Takeda A, Oku Y, et al. Stereotactic body radiotherapy for small hepatocellular carcinoma: a retrospective outcome analysis in 185 patients. *Acta Oncol*. 2014;53(3):399-404.
5. Toya R, Murakami R, Baba Y, et al. Conformal radiation therapy for portal vein tumor thrombosis of hepatocellular carcinoma. *Radiother Oncol*. 2007;84(3):266-271.

6. Bae SH, Jang WI, Park HC. Intensity-modulated radiotherapy for hepatocellular carcinoma: dosimetric and clinical results. *Onco-target*. 2017;8(35):59965-59976.

7. Toya R, Saito T, Shiraishi S, et al. Dose–function histogram evaluation using (99m)Tc-GSA SPECT/CT images for stereotactic body radiation therapy planning for hepatocellular carcinoma patients: a dosimetric parameter comparison. *Anticancer Res*. 2018;38(3):1511-1516.

8. Beppu T, Hayashi H, Okabe H, et al. Liver functional volumetry for portal vein embolization using a newly developed ^{99m}Tc-galactosyl human serum albumin scintigraphy SPECT-computed tomography fusion system. *J Gastroenterol*. 2011; 46(7):938-943.

9. Shimohigashi Y, Toya R, Saito T, et al. Tumor motion changes in stereotactic body radiotherapy for liver tumors: an evaluation based on four-dimensional cone-beam computed tomography and fiducial markers. *Radiat Oncol*. 2017;12(1):61.

10. Logan JK, Park PC, Wong FC, et al. Outcomes of patients with hepatocellular carcinoma and advanced cirrhosis after high-dose radiation therapy guided by functional liver imaging with Tc99m sulfur colloid liver SPECT-CT. *Int J Radiat Oncol Biol Phys*. 2016;96(2):e167-e168.

11. Tsegmed U, Kimura T, Nakashima T, et al. Functional image-guided stereotactic body radiation therapy planning for patients with hepatocellular carcinoma. *Med Dosim*. 2017;42(2):97-103.

12. Kai Y, Toya R, Saito T, et al. Plan quality and delivery time comparisons between volumetric modulated arc therapy and intensity modulated radiation therapy for scalp angiosarcoma: a planning study. *J Med Radiat Sci*. 2018;65(1):39-47.

13. Shioyama Y, Jang SY, Liu HH, et al. Preserving functional lung using perfusion imaging and intensity-modulated radiation therapy for advanced-stage non-small cell lung cancer. *Int J Radiat Oncol Biol Phys*. 2007;68(5):1349-1358.

14. Kida S, Bal M, Kabus S, et al. CT ventilation functional image-based IMRT treatment plans are comparable to SPECT ventilation functional image-based plans. *Radiother Oncol*. 2016;118(3):521-527.

15. Fukugawa Y, Namimoto T, Toya R, et al. Radiation-induced liver injury after 3D-conformal radiotherapy for hepatocellular carcinoma: quantitative assessment using Gd-EOB-DTPA-enhanced MRI. *Acta Med Okayama*. 2017;71(1):25-29.

16. Motosugi U, Ichikawa T, Sou H, et al. Liver parenchymal enhancement of hepatocyte-phase images in Gd-EOB-DTPA-enhanced MR imaging: which biological markers of the liver function affect the enhancement? *J Magn Reson Imaging*. 2009;30(5):1042-1046.